

REPORTS

 OPEN ACCESS



## Suitability of transiently expressed antibodies for clinical studies: product quality consistency at different production scales

Sara Rodriguez-Conde<sup>a</sup>, Sophie Inman<sup>b</sup>, Viv Lindo<sup>b</sup>, Leanne Amery<sup>c</sup>, Alison Tang<sup>d</sup>, Uche Okorji-Obike<sup>e</sup>, Wenjuan Du<sup>f</sup>, Berend-Jan Bosch<sup>g</sup>, Paul J. Wichgers Schreur<sup>g</sup>, Jeroen Kortekaas<sup>h</sup>, Isabel Sola<sup>i</sup>, Luis Enjuanes<sup>i</sup>, Laura Kerry<sup>e</sup>, Katharina Mahal<sup>e</sup>, Martyn Hulley<sup>d</sup>, and Olalekan Daramola<sup>a</sup>

<sup>a</sup>Cell Culture & Fermentation Sciences, BioPharmaceutical Development, BioPharmaceuticals R&D, AstraZeneca, Cambridge, UK; <sup>b</sup>Analytical Sciences, BioPharmaceutical Development, BioPharmaceuticals R&D, AstraZeneca, Cambridge, UK; <sup>c</sup>Late-Stage Formulation Sciences, BioPharmaceutical Development, BioPharmaceuticals R&D, AstraZeneca, Cambridge, UK; <sup>d</sup>Purification Process Sciences, BioPharmaceutical Development, BioPharmaceuticals R&D, AstraZeneca, Cambridge, UK; <sup>e</sup>Analytical Sciences, Bioassay Biosafety and Impurities, BioPharmaceutical Development, BioPharmaceuticals R&D, AstraZeneca, Cambridge, UK; <sup>f</sup>Virology Section, Infectious Diseases and Immunology Division, Department of Biomolecular Health Sciences, Faculty of Veterinary Medicine, Utrecht University, Utrecht, The Netherlands; <sup>g</sup>Department of Virology and Molecular Biology, Wageningen Bioveterinary Research, Lelystad, The Netherlands; <sup>h</sup>Boehringer Ingelheim Animal Health, Saint Priest, France; <sup>i</sup>Department of Molecular and Cell Biology, National Center of Biotechnology (CNB-CSIC), Campus Universidad Autónoma de Madrid, Spain

### ABSTRACT

Transgenic human monoclonal antibodies derived from humanized mice against different epitopes of the Middle East respiratory syndrome coronavirus (MERS-CoV), and chimeric llama-human bispecific heavy chain-only antibodies targeting the Rift Valley fever virus (RVFV), were produced using a CHO-based transient expression system. Two lead candidates were assessed for each model virus before selecting and progressing one lead molecule. MERS-7.7G6 was used as the model antibody to demonstrate batch-to-batch process consistency and, together with RVFV-107-104, were scaled up to 200 L. Consistent expression titers were obtained in different batches at a 5 L scale for MERS-7.7G6. Although lower expression levels were observed for MERS-7.7G6 and RVFV-107-104 during scale up to 200 L, product quality attributes were consistent at different scales and in different batches. In addition to this, peptide mapping data suggested no detectable sequence variants for any of these candidates. Functional assays demonstrated comparable neutralizing activity for MERS-7.7G6 and RVFV-107-104 generated at different production scales. Similarly, MERS-7.7G6 batches generated at different scales were shown to provide comparable protection in mouse models. Our study demonstrates that a CHO-based transient expression process is capable of generating consistent product quality at different production scales and thereby supports the potential of using transient gene expression to accelerate the manufacturing of early clinical material.

### ARTICLE HISTORY

Received 22 November 2021  
Revised 2 March 2022  
Accepted 8 March 2022

### KEYWORDS

CHO cells; transient gene expression; product quality attributes; scalability; MERS; coronavirus; RVFV; bunyavirus; virus; zoonosis

## Introduction

Traditionally, transient gene expression (TGE) has been the technology used for production of therapeutic glycoproteins at early drug development stages because it allows for rapid production of high-quality material.<sup>1</sup> This technology involves introducing plasmid DNA, which encodes the protein of interest, into mammalian cells. The cells then express the recombinant protein over a limited period of time, typically up to 14–21 days. Several methods are used to transfer plasmid DNA into mammalian cells for TGE. Some of the most common chemical agents used for transfection are calcium phosphate, polyethyleneimines (PEIs) and cationic lipids. In particular, PEIs are frequently used due to the high transfection efficiency and relatively low cost compared to lipid-based reagents. An alternative to chemical-based transfection is the use of electroporation methods, such as the MaxCyte® STX™ flow electroporation system. Using this approach, Steger *et al.* were able to produce 3.5 g of antibody from less than 3 L of culture.<sup>2</sup>

Although currently this technology has been tested only at shake flask culture scale, it has the potential to be scaled up to several liters in bioreactors.

The most appropriate expression host depends on the particular protein being expressed, but mammalian cells are preferred for the production of complex proteins due to their inherent capacity to perform post-translational modifications.<sup>3</sup> Two of the most commonly used mammalian cell lines are human embryonic kidney (HEK) and Chinese hamster ovary (CHO) cells.<sup>4</sup> Historically, both cell lines have been used to produce small amounts (milligrams to grams) of therapeutic proteins at early research stages. However, for manufacturing at later drug development stages, stable CHO cell lines are the preferred option due to their regulatory track record, capacity for high levels of protein expression, and successful scale-up to 10,000 L bioreactors.<sup>5</sup> Therefore, using CHO cells for TGE has the advantage of using the same host cell type that is eventually used for stable cell-line development.

This is important as, by maintaining the same host cell type from early development stages to manufacturing, product quality characteristics are more likely to be conserved.<sup>6</sup> Finally, using CHO cells has a lower risk of introducing human viruses in the process compared to using human cell lines.<sup>3</sup>

In the past two decades, remarkable advances in TGE technologies have led to an increase in titers from mg/L to g/L.<sup>1,7-9</sup> These improvements are attributable to the optimization of many variables, including transfection reagents, transfection media, expression vectors, cell lines, and cell culture processes.<sup>10</sup> In addition to these developments, having a scalable expression system is key to meeting the increasing demand for grams of recombinant proteins, such as monoclonal antibodies (mAbs), to be used in preclinical, biochemical, and biophysical studies.<sup>11</sup> Few studies covering the scale up of TGE processes in bioreactors have been reported, with most of this work published more than a decade ago and mainly using HEK293 cells.<sup>11-15</sup> Tyzack *et al.* were the first to demonstrate successful scale up of a PEI-mediated TGE process using CHO cells at an industrially relevant scale of 500 L.<sup>16</sup> In an initial run, they were able to scale up their process from 5 L in a rocking bioreactor to 500 L in a single-use bioreactor (SUB), achieving crude titers of 1.50 g/L and 0.83 g/L, respectively. The lower titers observed in the SUB compared to the 5 L rocking bioreactors were attributed to increased cell growth. This scalability problem was resolved by developing and evaluating a new transfection method, which resulted in comparable expression levels between the different scales.<sup>16</sup>

Recent advances in TGE yields and scale-ups have opened opportunities to evaluate this technology for manufacturing at later stages of drug development. For example, transiently produced material could be used for GLP toxicology studies, while a stable cell line is generated, thereby decreasing the time to clinical trials.<sup>17</sup> Other potential applications of TGE are the manufacturing of clinical-grade material as part of a rapid pandemic response or in the context of personalized medicines.<sup>17-19</sup> However, historical concerns around low productivity, batch-to-batch consistency and comparability of product quality attributes (PQAs) between transient and stable-derived material have prevented the use of TGE for manufacturing therapeutic proteins beyond preclinical research.

In this study, human mAbs derived from transgenic mice against different epitopes of the Middle East respiratory syndrome coronavirus (MERS-CoV)<sup>20</sup> and camelid-derived multimeric single-domain antibody complexes (hIgG1Fc-VHH fusions) against the Rift Valley fever virus (RVFV)<sup>21</sup> were used to explore the feasibility of using a CHO TGE platform to generate clinical-grade material as part of a pandemic response strategy (Innovative Medicines Initiative (IMI) grant agreement no. 115760). Here, we report the results of the evaluation of the AstraZeneca CHO-based transient expression system at different scales. The process was successfully scaled up from 15 mL in miniaturized bioreactors to 200 L in SUBs. The process was also assessed for batch-to-batch consistency, with results showing that PQAs were consistent between batches, production scales and as expected for mAbs.

## Results

### Phenotypic stability analysis in miniaturized bioreactors

Our transient host, CHO-G22, is a derivative of the CHOK1 cell line that has been engineered to enhance transient protein expression by co-expressing the Epstein-Barr virus nuclear antigen-1 (EBNA-1) and glutamine synthetase genes.<sup>7</sup> The use of a host that supports consistent expression levels is critical when scaling up any production process. Therefore, our first step was to assess the phenotypic stability of our CHO transient cell line. MERS-7.7G6, a human mAb targeting different epitopes of the MERS-CoV spike glycoprotein, was used as the model antibody. Cells were recovered from a cryopreserved bank and cultured up to 34 passages. Development cell banks were created at passages 18, 23, 29, and 34. Cells at the different passages were recovered and assessed in a scale down bioreactor model (Ambr<sup>®</sup> 15) to monitor the effects of cell age on TGE level and product quality.

Maximum viable cell densities (VCD) between 7.38 and  $9.27 \times 10^6$  cells/mL were achieved at the different cell ages. Viability at time of harvest was between 82% and 87% for all tested conditions (data not shown). Results also showed that all tested cell ages were comparable in terms of antibody expression and glycosylation profiles (Figure 1). Average yields between 0.85 g/L and 0.92 g/L were obtained at 8 days after transfection. Finally, results showed that product quality was also consistent across the tested cell ages (Table 1).

Results of the phenotypic stability study supported the selection of passage 18 as the cell bank to be used for the subsequent runs since this simulates the inoculum seed train for up to a 12,000 L scale run.

### Assessing the TGE process reproducibility at 5 L scale

MERS-7.7G6, as the model antibody, was used to demonstrate batch-to-batch consistency of the process. Therefore, four independent experiments were run for this molecule at 5 L scale. A second anti-MERS-CoV spike glycoprotein antibody, MERS-1.6C7, was also assessed at a 5 L scale in stirred tank reactors (STRs). Both antibodies were derived from MERS-CoV spike-immunized humanized mice and expressed as human IgG1 isotype antibodies.<sup>20</sup> Finally, two novel camelid-derived bispecific hIgG1Fc-VHH fusions targeting RVFV, RVFV-107-104, and RVFV-150-104, were assessed at a 5 L scale.<sup>21</sup> For these other three antibodies, duplicate reactors were run in parallel. Cultures were harvested at 8 or 12 days post-transfection.

An average maximum VCD of  $6.59 \pm 0.40 \times 10^6$  cells/mL was obtained for the different batches of MERS-7.7G6, whereas an average VCD of  $6.01 \pm 0.18$ ,  $7.04 \pm 0.44$ , and  $6.63 \pm 0.74$  cells/mL was obtained for the replicate runs of MERS-1.6C7, RVFV-107-104, and RVFV-150-104, respectively. Harvest viability was above 75% for all the runs. Average antibody titers of  $0.77 \pm 0.06$  g/L,  $0.19 \pm 0.02$  g/L,  $1.03 \pm 0.03$  g/L, and  $0.41 \pm 0.02$  g/L were obtained for MERS-7.7G6, MERS-1.6C7, RVFV-107-104, and RVFV-150-104, respectively. The expression titers were consistent between the different independent batches and replicate bioreactors. Titers were also as expected,

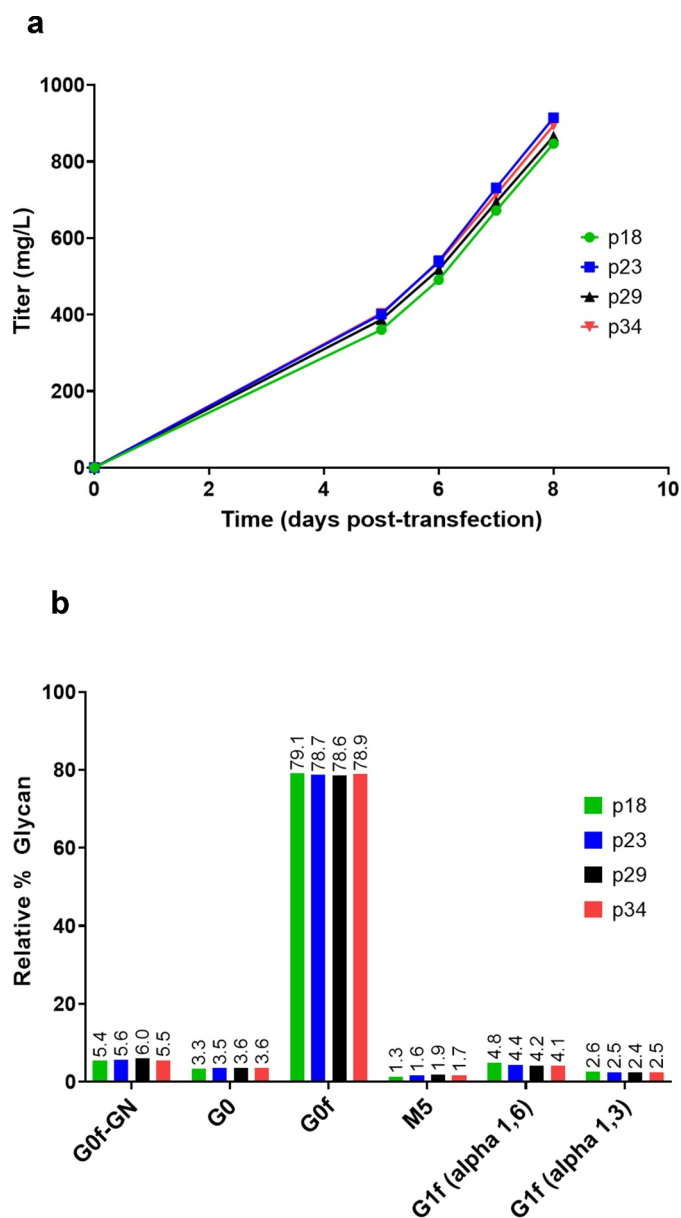


**Figure 1.** Consistency of antibody accumulation and N-linked glycosylation profiles at different cell ages. Duplicate vessels were transfected with plasmid DNA encoding MERS-7.7G6 in the Ambr<sup>®</sup> 15 system. Cultures were monitored for antibody expression (a) and purified material from the day 8 harvests was analyzed for glycosylation profile (b). Data shown is the average of the two replicate vessels except for p29 and p34 conditions where data for only one vessel is shown owing to instrument failure.

as they aligned with the previously observed data for these antibodies (data not shown). Rapid generation of material is essential during early stages of drug development. However, in scenarios, such as a pandemic response, maximizing yields is also critical to meet high drug dosage requirements. Therefore,

one of the runs of MERS-7.7G6 was extended to 12 days to determine maximum titers for this molecule. A yield of 1.74 g/L was obtained for this antibody when the process was extended compared to  $0.77 \pm 0.06$  g/L obtained for harvest on day 8.

Material from all the 5 L batches was harvested, purified, and analyzed. PQAs were found to be as expected for the mAbs and bispecific products, with no aggregation or fragmentation issues observed for any of the tested molecules (data not shown). Additionally, analytical results for MERS-7.7G6

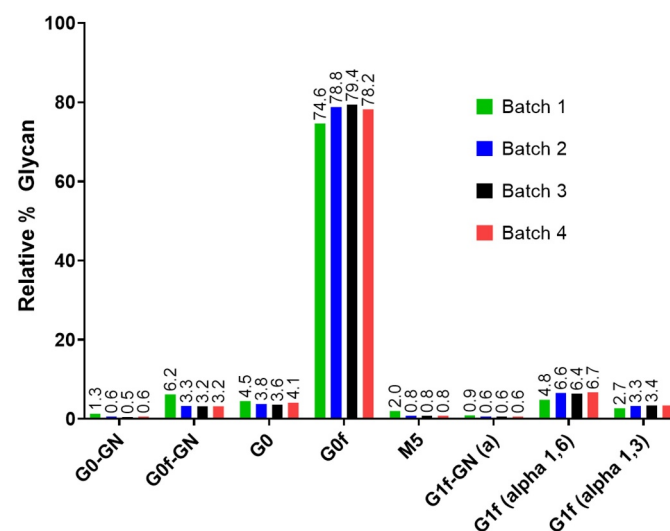


**Figure 2.** Glycosylation profile of four independent batches expressing MERS-7.7G6. 5 L bioreactors were transfected with plasmid DNA encoding a model anti-MERS antibody with four independent experiments run to determine batch-to-batch consistency of the transient process. Purified antibodies from the harvests were analyzed to assess glycan profiles. \*Note that batch 1 was harvested on day 12 while batches 2–4 were harvested on day 8.

showed consistent PQAs over the different batches (Figure 2 and Table 2), with minor differences observed in the level of the main G0f glycoform for material harvested after 12 days. The product quality results were also found to be comparable to those obtained for the Ambr<sup>®</sup> 15 cell age study described in the previous section.

### Scalability of the TGE process up to 200 L

To confirm the scalability of the transient process, the lead candidates against each of the two model viruses were scaled up. MERS-7.7G6 was scaled up to 50 L and 200 L SUBs while RVFV-107-104 was scaled up to a 200 L SUB. Bioreactors were

**Table 1.** Analytical results for MERS-7.7G6 produced at different cell passages.

	HPSEC % Monomer	cIEF cIEF main peak pl	cIEF % main peak	cIEF % acidic peaks	cIEF % basic peaks	Reduced CGE % purity	Non-reduced CGE % purity	Intact mass (Da)
Passage 18	99.6	8.8	72.8	19.2	7.9	98.4	94.8	149799
Passage 23	99.6	8.8	73.1	19.8	7.1	98.4	94.9	149799
Passage 29	99.4	8.8	71.9	19.4	8.7	98.3	94.8	149799
Passage 34	99.5	8.8	72.5	19.4	8.1	98.4	94.6	149799

Material from the duplicate Ambr<sup>®</sup> 15 vessels was pooled and purified. Purified antibody was analyzed by HP-SEC, cIEF, CGE, and LC/MS.

**Table 2.** Product quality data for the four batches of MERS-7.7G6.

	HPSEC % Monomer	cIEF cIEF main peak pl	cIEF % main peak	cIEF % acidic peaks	cIEF % basic peaks	Reduced CGE % purity	Non-reduced CGE % purity	Intact mass (Da)
Batch 1*	99.0	8.9	63.2	29.9	6.8	98.3	94.6	149799
Batch 2	99.5	8.7	69.6	20.2	10.2	98.5	95.9	149800
Batch 3	98.4	8.8	66.6	24.3	9.1	98.6	96.5	149800
Batch 4	100.0	8.8	68.3	20.1	11.6	98.3	96.2	149800
% RSD	0.7	0.9	4.1	19.5	21.5	0.2	0.9	0.0

Purified antibody was analyzed by HP-SEC, cIEF, CGE, and LC/MS. \*Note that batch 1 was harvested on day 12 while batches 2–4 were harvested on day 8.

sampled daily and harvested when viability was below 75% or on day 12. Material was purified and product quality analysis was performed for all batches.

For MERS-7.7G6, maximum VCD values of 8.63 and  $9.15 \times 10^6$  cells/mL were obtained at 50 L and 200 L scales, respectively, compared to an average maximum VCD of  $6.59 \pm 0.40 \times 10^6$  cells/mL obtained for the four runs at 5 L scale. Viability at time of harvest was between 73% and 81% for all three scales (data not shown). Yields of 0.81 g/L and 0.78 g/L were obtained at 8 days post-transfection in the 50 L and 200 L SUB, respectively. These results are comparable to those obtained at the Ambr<sup>®</sup> 15 and 5 L scales. When the process was extended to 12 days, maximum titers of 1.23 g/L and 1.15 g/L were obtained at 50 and 200 L scale, respectively, compared to 1.74 g/L obtained at 5 L scale. This is a decrease of 29% and 34% for the 50 and 200 L scales, respectively.

For RVFV-107-104, a maximum VCD of  $7.1 \times 10^6$  cells/mL was achieved in the 200 L SUB compared to an average of  $7.04 \pm 0.44 \times 10^6$  cells/mL at the 5 L scale. The 200 L SUB was harvested on day 9 because viability had dropped to 75%. Expression titers of 0.46 and 0.56 g/L were obtained at day 8 and 9, respectively, in the 200 L SUB. This is a titer decrease of 55% compared to the 5 L scale, which achieved  $1.03 \pm 0.03$  g/L on day 8. The unexpected low titer in the 200 L SUB is linked to lower cell viability and earlier harvest.

Regarding product quality for the larger scale runs, results were comparable to those obtained at a 5 L scale for both candidates, MERS-7.7G6 (Figure 3a and Table 3) and RVFV-107-104 (Figure 3b and Table 4), with only minor differences observed in the level of the main G0F glycoform for material harvested at different days.

For both candidates, peptide mapping was performed to further confirm the consistency of the PQAs. Figure 4 shows the UV chromatograms of the tryptic digests of MERS-7.7G6 and RVFV-107-104 material from the different production scales. Results show comparable results across scales. All peaks with a relative abundance greater than 1% of the base peak were identified as deriving from the expected sequence or tryptic autolytic peptides. The data suggest the absence of sequence variants arising from the TGE process or scale up for either of the two molecules.

### Evaluation of the functionality and neutralizing activity of purified antibodies in in-vitro and in-vivo assays

As a final confirmation that the material produced was functional and comparable across scales, both lead candidates were evaluated for neutralizing activity using *in vitro* and *in-vivo* assays. MERS-7.7G6 was evaluated in a binding assay,

pseudotyped virus neutralization assay and mouse models. RVFV-107-104 was assessed for binding to RVFV aminoterminal glycoprotein (Gn) by enzyme-linked immunosorbent assay (ELISA) and immunofluorescence assay (IFA) and for virus neutralizing activity by virus neutralization test (VNT).

Figure 5 shows the results of the binding and pseudoviral neutralization assays performed with MERS-7.7G6. Samples taken from the different scale-up batches were measured to determine the relative binding of each batch against the reference material (from a 5 L batch). All samples were within 20% relative binding of the reference standard (Table 5). For the neutralization of MERS-CoV infection, material from the 5 L and 200 L scale batches were tested using a previously established VNT.<sup>20</sup> The IC<sub>50</sub> titers of MERS-7.7G6 5 L and 200 L scale batches were comparable, and similar to IC<sub>50</sub> titer reported by Widjaja *et al.*<sup>20</sup>

To evaluate the efficacy of MERS-7.7G6, 49 K18 TghDpp4-transgenic mice (20–30 weeks-old) were administered, after inoculation with MERS-CoV, with the mAb or negative controls (Table 6). Based on the inherent variability of this model and protection previously reported, 80–100% survival is regarded as protection.<sup>20,22</sup> The results indicated that MERS-7.7G6 mAb, independent of the production scale, protected the mice when administered after virus inoculation (Figure 6).

Finally, to assess the *in vitro* potency of the RVFV-107-104 mAb, purified material from the different scales was tested in ELISAs. The results confirmed nM-range binding that was comparable across the different scales (Figure 7a). IFA subsequently confirmed efficient recognition of native RVFV antigen (Gn in infected cells [Figure 7b]). Furthermore, a highly sensitive VNT, based on a four-segmented RVFV expressing eGFP from the NSs locus (RVFV-4s-eGFP) (Figure 7c), confirmed potent neutralization in the nM range that was also comparable between the different scales (Figure 7d).

## Discussion

Over the past two decades, the productivities of TGE in CHO cells have dramatically increased. In addition, the scale up of different TGE processes in both CHO and HEK cells to industrially relevant volumes have been reported.<sup>15,16</sup> These advances have the potential to reduce the time for drug development, as transiently generated material could be used to manufacture therapeutic proteins for toxicology studies or even directly given to patients in a pandemic rapid response scenario.<sup>17</sup> However, historical concerns associated with transient gene expression (e.g., low yields, batch-to-batch consistency) have prevented the use of this technology at later stages of drug development. In addition to this, there are several factors that

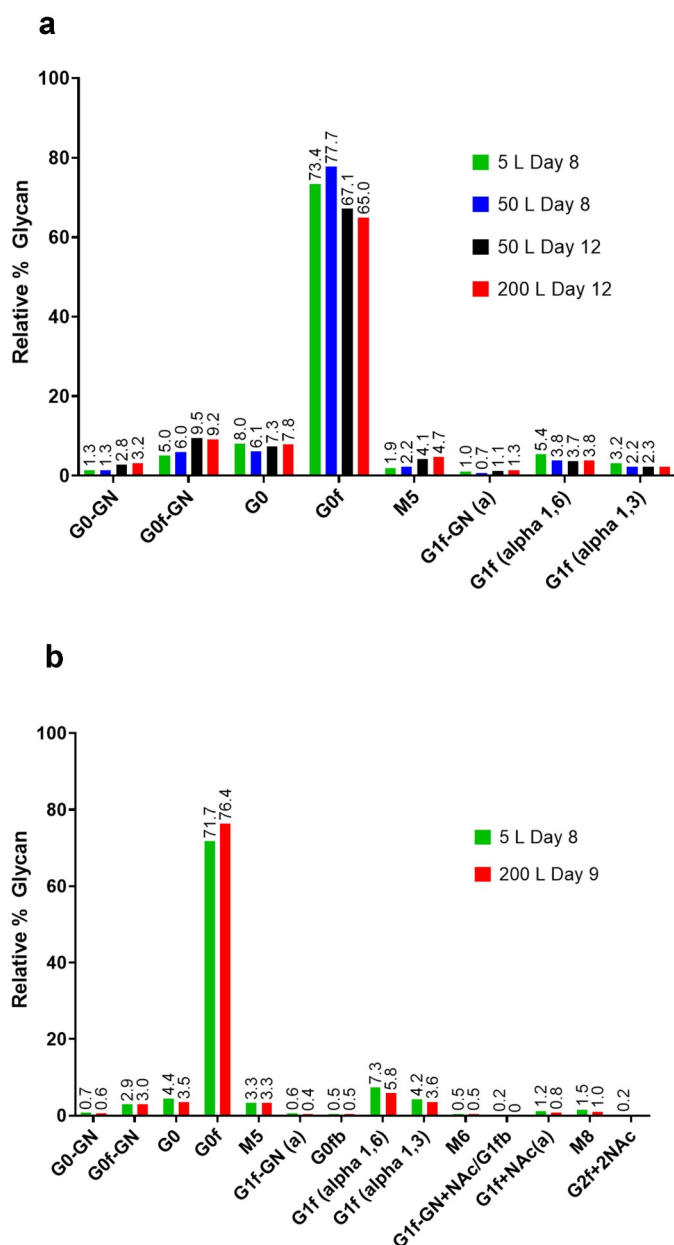


**Figure 3.** Glycosylation profiles observed for MERS-7.7G6 (a) and RVFV-107-104 (b) manufactured at 5, 50 and 200 L scales. The 5 L batches for both molecules were harvested on day 8. The larger scale runs were extended to 12 days for MERS-7.7G6 and 9 days for RVFV-107-104. A single experiment at 50 and 200 L scales was run. Samples were taken after 8 and 12 days from the MERS-7.7G6 50 L scale. Purified antibodies were analyzed to assess glycan profiles.

should be considered if TGE is used beyond preclinical research. TGE requires large amounts of plasmid DNA, so the potential impact on the economics and timelines of the

process will need to be managed. The expression levels of TGE may still be a limiting factor, especially when high drug doses are required. Furthermore, specific assays may be required to confirm clearance of transient host-specific and process-related impurities, such as the transfection reagent PEI. Comparability studies are required if transiently expressed material is used for first-in-human studies and stably expressed material is used for later clinical studies. However, this can be mitigated by product-quality-driven clone selection to ensure comparability between the two platforms. Finally, current regulatory requirements have restricted the use of TGE for drug manufacturing,

**Table 4.** Product quality data for RVFV-107-104 at 5 and 200 L scales.

Batch	HPSEC % Monomer	cIEF main peak pl	cIEF % main peak	cIEF % acidic peaks	cIEF % basic peaks	Reduced CGE % purity	Non-reduced CGE % purity
5 L D8	98.9	8.6	58.9	39.5	1.6	91.3	99.7
200 L D9	99.2	8.6	56.1	42.0	1.9	97.0	99.6

Purified antibody complex was analyzed by HP-SEC, cIEF, CGE, and LC/MS. Note that the 5 L reactor was harvested at 8 days post-transfection while the 200 L reactor was harvested 9 days post-transfection.

as the latest guidelines from the U.S. Food and Drug Administration (FDA) specifically state the requirement of a cloning step for generation of a master cell bank.<sup>9</sup>

As part of the Zoonoses Anticipation and Preparedness Initiative (ZAPI, IMI grant agreement no. 115760), the aim of this study was to assess the feasibility of using a TGE platform for manufacturing antibodies in response to a potential pandemic. In addition to evaluating production at an industrially relevant manufacturing scale, we also assessed batch-to-batch product quality consistency. This addressed one of the key concerns of using material produced from different transient expression runs. To mimic manufacturing volumes of up to 12,000 L, we investigated the phenotypic stability of the cell host by assessing expression level and product quality at different cell ages for a model mAb (MERS-7.7G6) in a miniaturized bioreactor (Ambr<sup>®</sup> 15). The data confirmed consistent expression levels and product quality from passage 18 to passage 34. Scale-up and process consistency were thereafter assessed at a 5 L scale in bench-top bioreactors for the lead antibodies. Two antibodies, MERS-7.7G6 and RVFV-107-104, showed promising expression levels, with titers of  $0.77 \pm 0.06$  g/L and  $1.03 \pm 0.03$  g/L at 8 days post-transfection, respectively. However, the two back-up antibodies, MERS-1.6C7 and RVFV-107-150, showed lower expression levels, with titers of  $0.19 \pm 0.02$  g/L and  $0.41 \pm 0.02$  g/L at

**Table 3.** Product quality data for MERS-7.7G6 at 5, 50 and 200 L scales.

Batch	HPSEC % Monomer	cIEF main peak pl	cIEF % main peak	cIEF % acidic peaks	cIEF % basic peaks	Reduced CGE % purity	Non-reduced CGE % purity	Intact mass (Da)
5 L D8	100.0	8.8	65.2	22.0	12.9	98.7	96.6	149800
5 L D12	99.3	8.8	62.4	29.0	8.6	98.3	95.0	149798
50 L D8	99.1	8.7	62.3	27.9	9.7	98.4	95.4	149804
50 L D12	99.0	8.7	59.0	32.1	8.9	97.6	94.7	149804
200 L D12	99.3	8.7	68.3	22.2	9.5	95.5	98.8	149801
% RSD	0.4	0.6	5.5	16.6	17.4	1.3	1.7	0.0

Purified antibody from day 8 (D8) or day 12 (D12) harvests was analyzed by HP-SEC, cIEF, CGE, and LC/MS.

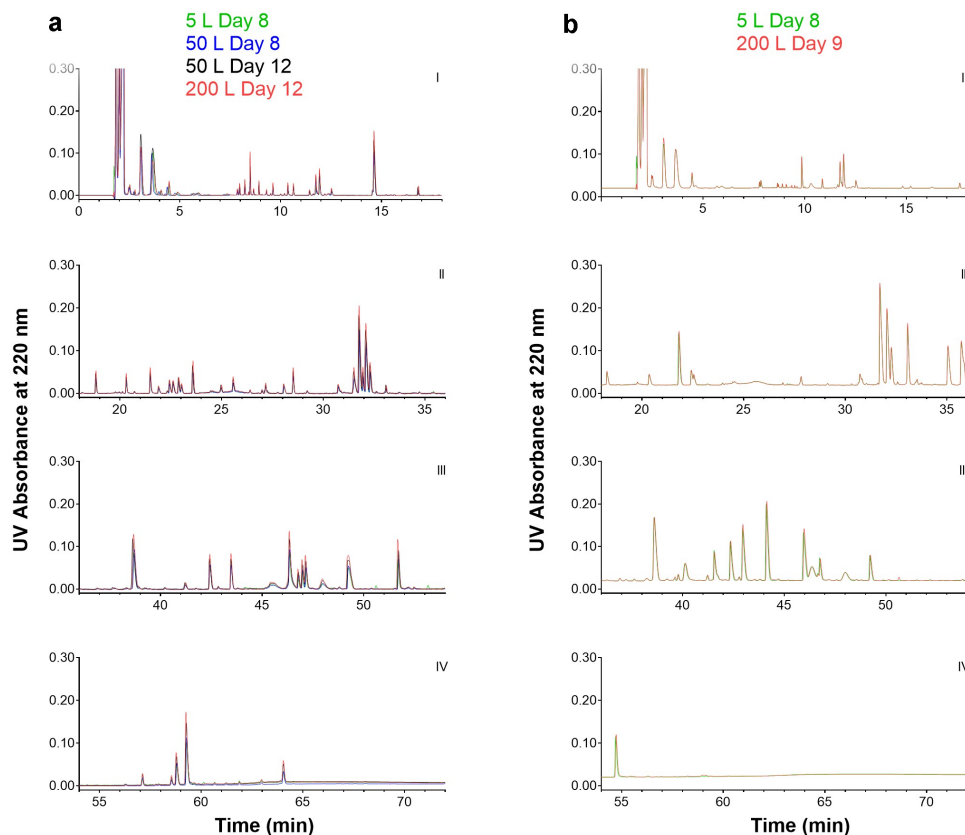


**Figure 4.** Overlay of UV chromatograms of peptide mapping of MERS-7.7G6 (a) and RVFV-107-104 (b) at different scales and harvest days.

8 days, respectively. The lower expression of these antibodies was consistent with the productivities observed during the early stages of the project (data not shown). Different expression levels for different antibodies of the same format are not unusual and have been previously reported.<sup>23</sup> Further work, such as gene sequence optimization, could be performed to improve expression. However, here the lower-expressing leads were down-selected based on a combination of potency and expression data.

Process consistency was evaluated in a 5 L stirred-tank reactor using MERS-7.7.G6 as the model antibody. Four independent runs for this antibody were carried out, resulting in an average maximum VCD of  $6.59 \pm 0.40 \times 10^6$  cells/mL and an average titer of  $0.77 \pm 0.06$  g/L at 8 days post-transfection. PQAs were found to be consistent between the different batches and within the typical expected ranges for mAbs. These data confirm that a TGE process can be developed and controlled to enable product quality consistency from different batches, which is critical for preclinical and clinical studies. The success of gene transfer to cells and subsequent expression is affected by the quality of the plasmid DNA; for example, levels of supercoiled plasmid DNA and microbial impurities can affect expression. Therefore, plasmid DNA product quality should be monitored and controlled. As higher levels of supercoiled plasmid have a positive effect on expression, chromatographic processes have been developed to efficiently purify supercoiled conformation plasmid from open circular and linear isoforms.<sup>24</sup> The levels of the different plasmid DNA isoforms can be determined by capillary gel electrophoresis,

whilst other assays can be used to monitor levels of impurities, such as microbial proteins, RNA, genomic DNA, and endotoxin. It is notable that the FDA recommends establishing a minimum specification for supercoiled plasmid content (preferably >80%) for plasmid DNA vaccines.<sup>25</sup>

To assess the impact of scale on titer and product quality, the two lead candidates were scaled up to 50 L and/or 200 L SUBs. For MERS-7.7G6, comparable titers to those reported for the 5 L STR were obtained in the two SUBs on day 8. However, when the process was extended to 12 days, 29% and 34% drops in expression yields were observed at 50 L and 200 L scales, respectively. An even larger drop in expression level (55%) was observed for RVFV-107-104 at 200 L scale attributable to the lower viabilities observed in the SUB. The reduced yield at higher scales was not unexpected, as maintaining productivities is one of the main challenges during bioprocess scale up. This highlights the need for process optimization where different factors, such as culture mixing, heat and gas transfer rates and transfection protocol, should be assessed, with the aim of increasing expression yields at scale.

During scale up, not only is high productivity desirable, but good and consistent final product quality is also essential because changes in charge variants and glycosylation profiles can occur during process transfer.<sup>26</sup> Although the productivities were lower at the 50 and 200 L scales, the PQAs for the two lead antibodies were found to be quite consistent across the different scales. The 2-aminobenzamide (2-AB) data showed that G0F is the predominant glycoform, which aligns with the glycan profile reported for stable cell lines derived from the

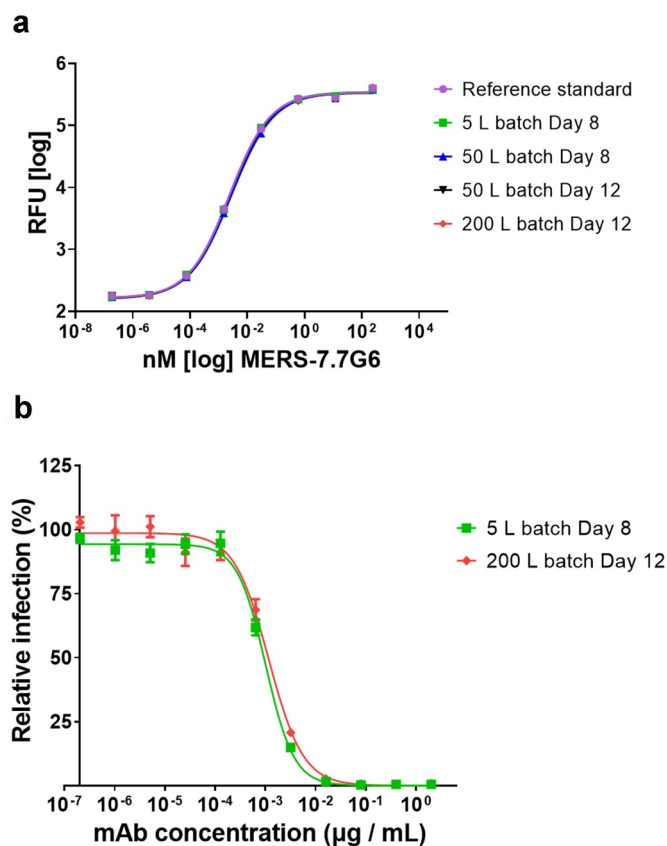


**Figure 5.** Binding efficiency of MERS-7.7G6 antibody (a). Material from different batches was tested as a measure of product quality (S1 spike protein binding assay). Neutralization of MERS-CoV infection (b). Material from 5 L and 200 L scale batches of MERS-7.7G6 was tested using a previously established pseudoviral assay.<sup>20</sup> Luciferase-encoding VSV particles pseudotyped with the MERS-CoV spike protein and pre-incubated with the antibodies at indicated concentrations were used to infect Vero-CCL81 cells. At 20 h post infection, luciferase activity was determined in cell lysates to calculate infection (%) relative to mock-treated virus controls. The average of six replicates is shown.

same parent CHO host.<sup>27,28</sup> Capillary gel electrophoresis (CGE) data showed that extending our transient process from 8 to 12 days had no significant effect on purity levels or charge profile and glycan composition was broadly similar with only small differences in G0F levels. The minor differences in G0F level is thought to be linked to the different harvest days, as this effect has been previously reported although the underlying cause is unknown.<sup>9,29</sup> In addition, glycosylation profiles can be affected by multiple factors, such as the cell host, expressed mAb, culture media, and bioreactor process conditions.<sup>30</sup> Therefore, all these parameters should be carefully considered and defined when setting process parameters for TGE processes to ensure batch-to-batch product quality consistency.

**Table 5.** Binding assay results for MERS-7.7G6 at different scales.

Batch	Assay #1 (%)	Assay #2 (%)	RP (%) GEOMEAN	Natural log (LN) of RP #1	Natural log (LN) of RP #2	STDEV of LN	% GCV
5 L D8	92	100	96	4.52	4.61	0.059	6.1
50 L D8	78	85	81	4.36	4.44	0.061	6.3
50 L D12	88	87	87	4.48	4.47	0.008	0.8
200 L D12	84	98	91	4.43	4.58	0.109	11.5

Raw values were modeled to a 4-parameter logistic fit, and analyses were run using Qubas software from Quantics. Two independent assays were run to provide two results for each sample from which a reportable result was calculated (% relative binding to reference standard).

To confirm the functionality of the material generated at the different scales, the two lead antibodies were tested for neutralizing activity. MERS-7.7G6 was tested in *in-vitro* assays and *in-vivo* mouse models. Results showed that MERS-7.7G6, independent of production scale, was able to neutralize the MERS-CoV in a pseudotyped VNT. The results of the *in-vivo* protection studies were in alignment with previously reported percentage survival for MERS-7.7G6 where 80–100% percentage survival is

**Table 6.** Summary mAbs included in the mouse protection assay.

mAb	Production scale	Dose* (mg/kg target)	Administration	N° of mice
MERS-7.7G6	200 L SUB	10	Post-infection	11
MERS-7.7 G6	5 L STR	10	Post-infection	11
Isotype control	N/A	10	Post-infection	11
Mock infected	N/A	–	No mAb	5

\*dose used corresponds to ~50 µg/mouse.

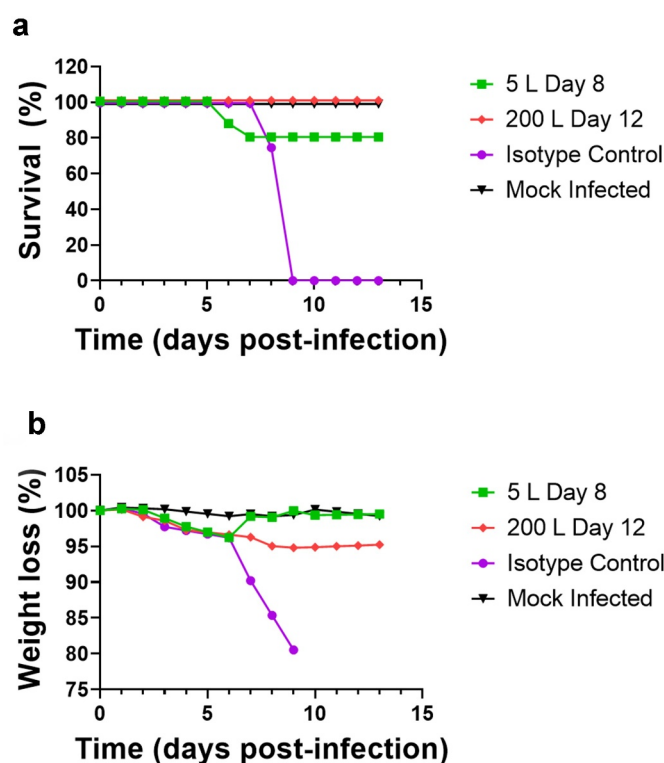


**Figure 6.** Survival and weight loss of mice infected with MERS-CoV. To evaluate the efficacy of the MERS-7.7G6 mAb, K18 hDPP4-transgenic mice (20–30 weeks-old) were administered, after inoculation with MERS-CoV (5000 pfu/mouse), with the selected mAb or negative controls (10 mg/Kg dose). Based on the inherent variability of this model and protection previously reported, 80–100% survival is regarded as protection.

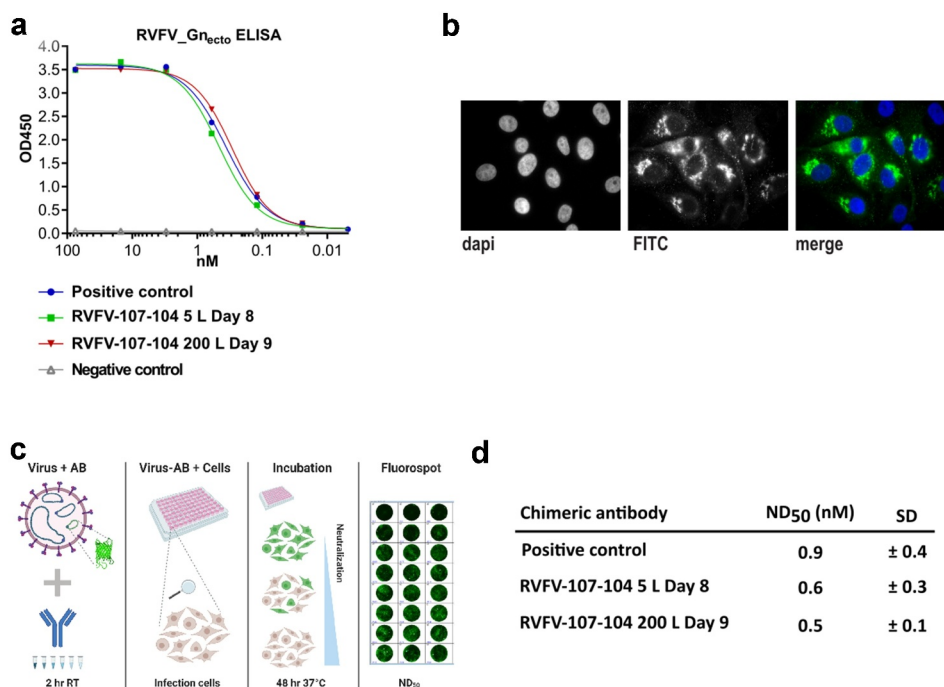


**Figure 7.** *In-vitro* potency of RVFV-107-104 antibody. Indirect RVFV-Gn<sub>ecto</sub>-based ELISA (a). IFA of the using RVFV-Clone 13 infected cells as antigen (b). Illustration of the VNT used to assess RVFV neutralization (c). Neutralizing activity of the purified chimeric antibody expressed as ND<sub>50</sub> (d).

considered as protection. Different batches of RVFV-107-104 were also analyzed using a panel of *in-vitro* assays (ELISA, IFA, and VNT). The results confirmed that the material generated at the different scales efficiently recognized the native RVFV Gn protein to have potent neutralizing activity.

In summary, we successfully demonstrated that our CHO-based TGE system is capable of generating antibodies of consistent product quality at different scales and in different batches. Furthermore, *in-vitro* and *in-vivo* data confirmed the consistent activity and potency of the different batches of material. We have also shown that PQAs of the material generated were within the ranges typically expected for mAbs. To our knowledge, this is the first study that has investigated product quality variability at different scales and batches for transiently expressed material. An area of interest for future work is a more detailed product quality comparison between the transiently generated material and material produced in stable cell lines (pools or clonal cell lines), which was beyond the scope of this study. Finally, in addition to the recently reported accelerated timelines for stable pools and stable clones,<sup>17,18,31</sup> our data suggest that, subject to regulatory approval, TGE can be considered as a potential alternative platform to rapidly generate high-quality material that could be used for clinical studies, especially for first-in-human studies or/and to support a pandemic response. The selection of TGE over pools as a rapid production system depends on the drug development strategy. Although TGE requires large amounts of plasmid DNA, a fully established plasmid DNA production process integrated into the TGE timelines, i.e., plasmid production taking place in parallel with the cell bulk-up stages, may still have time savings over a stable pool strategy. A further advantage of using TGE is that the cell bank only

needs to be characterized once, and this time-consuming safety testing can be performed off the critical path for large-scale manufacture. In contrast, a stable pool approach requires cell bank testing for each product and can be a bottleneck for rapid manufacturing.

## Materials and methods

### Cell culture and expression plasmids

CHO-G22 is a derivative of the CHOK1 cell line (ECACC No: 85051005). This cell line was engineered to enhance transient protein expression by co-expressing the Epstein-Barr virus nuclear antigen-1 (EBNA-1) and glutamine synthetase genes. Cells were maintained in AZ proprietary medium supplemented with methionine sulfoximine (MSX; Merck, product ref. #M5379-500) and hygromycin (Sigma, product ref. #10687010). Cultures in Erlenmeyer flasks or roller bottles were incubated at 140 rpm in a humidified orbital shaking incubator at 36.5°C and 5% CO<sub>2</sub>.

The expression plasmids are based on the Gahn and Sugden report, with transcription of the antibody genes driven by the human cytomegalovirus promoter.<sup>32</sup> For the production of the plasmids, the *E. coli* DH5α strain was used. Plasmids were purified using a commercial kit (Qiagen, product ref. # 12191) according to the manufacturer's instructions. Expression vectors encoding the following antibodies were assessed in TGE: MERS-7.7G6 (human IgG1), MERS-1.6C7 (human IgG1), RVFV-107-104 (llama bispecific single-domain antibody with human IgG1 Fc), RVFV-150-104 (llama bispecific single-domain antibody with human IgG1 Fc).



### **Transient expression in bioreactors**

Cells were grown in three systems: Ambr® 15 microbioreactor, 5 L STR and SUB at 50 L and 200 L scales. Bioreactors were seeded at  $2 \times 10^6$  viable cells/mL. After 24 h, cells were transfected with 1 mg of DNA per liter of culture volume using PEI<sub>max</sub> (PolySciences, product ref. #24765) as transfection reagent at a PEI:DNA ratio of 6:1 or 7:1. PEI and DNA were each diluted in 150 mM NaCl before being combined to form the DNA-PEI complex. Post-transfection, cultures were maintained at 37°C for 4 h and then temperature was reduced from 37°C to 34°C. The transfected cells were fed with AZ proprietary nutrient supplement over the course of the culture period. Cultures were maintained at 34°C, 50% DO, pH 7 for 8–12 days. VCD, total cell density, and viability were measured using a Vi-Cell XR cell counter (Beckman Coulter). Off-line pH, pO<sub>2</sub>, pCO<sub>2</sub> and glucose and lactate concentrations were quantified using a Nova Bioprofile FLEX (Nova Biomedical).

### **Antibody quantification and purification**

Antibodies in cell culture supernatants were quantified by protein A high-performance liquid chromatography (HPLC) on an Agilent 1200 HPLC (Agilent Technologies, Cheshire UK) by comparing eluate peak size from each sample with a calibration curve. Larger volumes of cell culture were clarified with a Millistak+ D0HC and X0HC (Millipore, Watford) depth filter train. Clarified material was loaded on a Prisma (GE Healthcare, Buckinghamshire) Protein A affinity column equilibrated in 50 mM Tris pH 7.4, the columns were washed with 50 mM Tris pH 7.4 followed by 50 mM Tris, 50 mM sodium caprylate pH 9.0 and 50 mM Tris pH 7.4. The proteins were eluted with 25 mM sodium acetate pH 3.6. The Protein A chromatography product was adjusted to pH 2.5 and held for 30 min before being neutralized to pH 7.4. The neutralized product was further purified using a Mustang Q (Pall, Portsmouth) anion exchange membrane chromatography column operated in flow-through mode. The anion exchange product was then buffer exchanged into the proprietary final formulation using tangential flow filtration using a Pellicon XL ultracel membrane (Millipore, Watford).

### **Product quality analysis**

#### **Charge variant analysis: cIEF**

Capillary isoelectric focusing was performed using an iCE3 Analyzer. Samples were adjusted to 0.5 mg/mL using a 4 M urea master mix containing methyl cellulose and 3–10 Pharmalytes. The samples were loaded onto an iCE3 Analyzer and focused for 15 min.

#### **Fragment analysis: CGE**

CGE was performed under both reducing and non-reducing conditions. For reduced CGE, samples were diluted to 1 mg/mL using a reducing buffer containing  $\beta$ -mercaptoethanol and sodium dodecyl sulfate. For non-reduced CGE, sample was diluted to 1 mg/mL in non-reducing sample buffer containing N-ethyl maleimide in sodium phosphate and sodium dodecyl

sulfate. Reduced and non-reduced samples were heat denatured at 65°C prior to analysis. Analysis was performed on a PA800 plus configured with a 30 cm bare fused silica capillary.

#### **Purity and aggregate analysis: HP-SEC**

High-performance size-exclusion chromatography (HP-SEC) with detection by absorbance at 280 nm was performed on a Tosoh TSK-gel G3000SWxL column (7.8 mm  $\times$  30 cm) at room temperature (RT). Samples were eluted isocratically with a mobile phase composed of 0.1 M sodium phosphate, 0.1 M sodium sulfate, pH 6.8 at a flow rate of 1.0 mL/min.

#### **Mass analysis**

Liquid chromatography coupled to high-resolution mass spectrometry (LC-HRMS) of the analyte was used to characterize the primary and quaternary structure of the analyte, as well as to determine the glycosylation profile. Reverse phase LC was coupled directly to a Synapt G2 (Waters) operated in positive ion, sensitivity mode. Data analysis was performed in MassLynx 4.1 using the MaxEnt1 algorithm for deconvoluted mass calculations.

#### **Primary structure analysis: reduced peptide mapping**

Peptide mapping was used to characterize the primary structure and any post-translational modifications of the proteins. Tryptic peptide mapping was performed by LC-HRMS. Samples were denatured and reduced by incubation with dithiothreitol and diluted to 5 mg/mL with water. Alkylation was performed by addition of iodoacetamide followed by incubation at RT in the dark. Samples were desalted by microdialysis. Protein digestion was performed by addition of a 0.67  $\mu$ g/ $\mu$ L trypsin solution in 100 mM Tris pH 7.5. Digestion was for 4 hours at 37°C before reaction quenching with trifluoroacetic acid (TFA). The resulting peptide mixtures were then separated by UPLC-MS using a Waters Acquity UPLC system equipped with a Waters Acquity BEH C18 column and an aqueous TFA/acetonitrile gradient. Mass measurements were performed on an Q Exactive HF-X Hybrid Quadrupole-Orbitrap mass spectrometer.

#### **Glycan analysis: 2-AB**

2-AB-labeled oligosaccharides analysis was performed following N-linked oligosaccharides digestion with Peptide-N-Glycosidase F. The released oligosaccharides were labeled with 2-AB by reductive amination. The labeled oligosaccharides were separated by UPLC on an Acquity UPLC with BEH Glycan column.

### **In vitro functional testing of MERS-7.7G6**

#### **Binding assay**

The relative binding of MERS-7.7G6 antibody was measured by using an electrochemiluminescence sandwich assay (Meso Scale Discovery technology, MSD). S1 spike protein was coated on assay plates at a fixed concentration and incubated overnight. MERS7.7G was added as a serial dilution followed by a fixed concentration of anti-human IgG sulfo-tag secondary antibody (MSD, product ref. #D20JL-6). Raw data values were generated by reading on an MSD plate reader and analysis was

performed using a 4-parameter logistic fit from which relative-binding percentages between reference standard and samples were generated using EC50 values.

### **Virus neutralization test using pseudotyped VSV**

The production of MERS-CoV spike pseudotyped vesicular stomatitis virus (VSV) and neutralization test was performed as described by Widjaja et al.<sup>20</sup> HEK 293 T cells (~75% confluency) were transfected with the pCAGGS expression vector encoding the MERS-CoV spike protein with a C-terminal cytoplasmic tail truncation to increase cell surface expression levels. Forty-eight hours post-transfection, cells were infected with VSV-G-pseudotyped VSVΔG bearing the firefly (*Photinus pyralis*) luciferase reporter gene at a multiplicity of infection (MOI) of 1. Twenty-four hours later, supernatants were harvested and filtered through a 0.45 μm membrane. In the VNT, serially diluted mAbs were pre-incubated with an equal volume of virus at RT for 1 h, after which the mixture was added to Vero-CCL81 cells, and further incubated at 37°C. After 20 h, cells were washed once with phosphate-buffered saline (PBS) and lysed with cell lysis buffer (Promega). The expression of firefly luciferase was measured on a Berthold Centro LB 960 plate luminometer using D-luciferin as a substrate (Promega). The percentage of infectivity was calculated as the ratio of luciferase readout in the presence of mAbs normalized to luciferase readout in the absence of mAb. The half maximal inhibitory concentrations (IC50) were determined using 4-parameter logistic regression (GraphPad Prism v7.0).

### **In vitro functional testing of RVFV-107-104**

#### **Viruses, cells, and media**

Culture media and supplements were obtained from Gibco (Life Technologies, Paisley, United Kingdom) unless indicated otherwise. Virus stocks of RVFV strain Clone 13<sup>33</sup> were obtained after infections at low MOI (0.01) of Vero E6 cells (ATCC CRL-1586, Teddington, United Kingdom). Vero cells were maintained in Eagle's minimal essential medium supplemented with 1% nonessential amino acids, 1% antibiotic/antimycotic and 5% fetal bovine serum, at 37°C with 5% CO<sub>2</sub>. Cells were regularly tested for the absence of mycoplasma.

#### **ELISA**

The RVFV Gn soluble ectodomain (RVFV-Gnhead), expressed with an N-terminal Twin-Strep-tag,<sup>21</sup> was coated on Strep-Tactin® microplates (Cat. No. 2–1501-001, IBA). To this end, 100 μL/well of 0.3 μg/mL, in ELISA binding buffer (25 mM Tris-HCl, 2 mM EDTA, 140 mM NaCl, pH 7.6) was incubated for 2 h at RT. The plates were washed with PBS supplemented with 0.05% Tween-20 using an ELISA washer (6 pulses). Plates were blocked with 300 μL/well of ELISA blocking buffer (2% w/v skimmed milk in PBS supplemented with 0.05% Tween-20) for 1 h at RT. Plates were subsequently incubated with 100 μL/well of a five-fold dilution of hIgG1Fc-VHH fusions in blocking

buffer for 1 h at RT and then washed with the ELISA washer. Horseradish peroxidase (HRP)-conjugated goat anti-llama IgG-H + L (A160-100P, Bethyl, Montgomery, Texas) diluted 1:2,000 in blocking buffer (100 μL/well) was used as a secondary antibody (1 h at RT). TMB One Component HRP Microwell Substrate (TMBW 1000-01, SurModics, Minnesota) was added as a substrate.

#### **Immunofluorescence assay**

Vero E6 cells ( $3 \times 10^4$  cells/well) were seeded in a CultureWell 16 removable chambered coverglass (Grace Bio-Labs) and incubated with RVFV Clone 13 at MOI 0.1. Following overnight incubation at 37°C and 5% CO<sub>2</sub>, cells were fixed with 4% (v/v) paraformaldehyde for 15 min at RT and permeabilized with 1% (v/v) Triton X-100 for 5 min at RT. After one wash with PBST20, wells were subsequently blocked with IFA blocking buffer (5% (v/v) horse serum in PBS) and incubated for 1 h at 37°C. Diluted hIgG1Fc-VHH fusions (1 μg/mL) in blocking buffer (100 μL/well) were added and incubated for 1 h at 37°C. Following three washes with PBST20, a fluorescein isothiocyanate-conjugated goat anti-llama IgG H + L secondary antibody (Bethyl, A160-100 F) in blocking buffer (1:200, 100 μL/well) was added for 1 h at 37°C. Following incubation, the wells were washed again three times with PBST20, and submerged in VectaShield antifade mounting medium H-1000 (Vector Laboratories). Images were taken on an inverted widefield fluorescence microscope Axio Observer 7 (ZEISS, Germany) using appropriate filters and a 1.3 NA 100x EC Plan-NEOFLUAR oil objective in combination with an AxioCam MRm CCD camera and ZEN 2.6 Pro software (ZEISS, Germany).

#### **Virus neutralization test**

RVFV neutralization was assessed with the use of a highly sensitive VNT as described.<sup>34</sup> Briefly, in standard 96-well cell culture plates, 50 μL of three-fold serial dilutions of hIgG1Fc-VHH fusions (starting at 75 nM) were incubated with 50 μL of a 103.6 TCID<sub>50</sub>/mL RVFV-4s\_eGFP for 1.5 h at RT. Following addition of  $1.5 \times 10^4$  BHK-21 cells/well plates were incubated for 48 h at 37°C with 5% CO<sub>2</sub>. Plates were subsequently fixed with 4% paraformaldehyde (15 min RT) and after a final wash step with PBS, the neutralization capacity was calculated as ND50 using the AID vSpot Spectrum (Strassberg, Germany).

#### **Protection assay of MERS-CoV inoculated mice**

To evaluate the efficacy of the selected mAbs, 38 K18 TghDpp4-transgenic mice 20–30 weeks-old were administered after inoculation with MERS-CoV (5000 pfu/mouse), with the mAbs or negative controls. Mice were monitored daily for weight loss and survival. At selected intervals (0, 3, 6, and 10 days after inoculation), mice were blood-sampled. Three mice were sacrificed at 3 and 6 days post-inoculation to collect lungs for viral titer (by plaque assay or qPCR) and histopathology and histochemistry (data not shown). This study received approval from the ethics

committee at the National Center of Biotechnology (CNB-CSIC).

Audonnet (Boehringer Ingelheim Animal Health, Global Innovation, France; ZAPI coordinator).

## Abbreviations

2-AB	2-Aminobenzamide
ADCC	antibody-dependent cellular cytotoxicity
AZ	AstraZeneca
BHK	baby hamster kidney cell
CGE	capillary gel electrophoresis
CHO	Chinese hamster ovary
cIEF	capillary isoelectric focusing
EBNA-1	Epstein-Barr virus nuclear antigen-1
EC50	half maximal effective concentration
eGFP	enhanced green fluorescent protein
ELISA	enzyme-linked immunosorbent assay
Fc	fragment crystallizable
FDA	United States Food and Drug Administration
GLP	good laboratory practice
Gn	aminoterminal glycoprotein
HEK	human embryonic kidney
hlgG1	human immunoglobulin G1
HP-SEC	high performance size-exclusion chromatography
HRP	horseradish peroxidase
IC50	half-maximal inhibitory concentration
IFA	immuno fluorescence assay
LC-HRMS	high resolution mass spectrometry
mAb	monoclonal antibody
Man5	mannose 5
MERS-CoV	Middle East respiratory syndrome coronavirus
MSD	Meso Scale Discovery
MSX	L-Methionine sulfoximine
MOI	multiplicity of infection
ND50	fifty percent neutralizing dilution
PBS	phosphate buffered saline
PEIs	polyethylenimines
pfu	plaque-forming units
pl	isoelectric point
PQAs	product quality attributes
qP	specific productivity
qPCR	real-time polymerase chain reaction
reversed-phase LC/MS	liquid chromatography-mass spectrometry
RT	room temperature
RVFV	Rift Valley fever virus
STR	stirred tank reactor
SUB	single use bioreactors
TCID	fifty-percent tissue culture infective dose
TFA	trifluoroacetic acid
TGE	transient gene expression
TMB	3,3',5,5'-Tetramethylbenzidine
Tris	tris(hydroxymethyl)aminomethane
UPLC	ultra performance liquid chromatography
UV	ultraviolet
VCD	viable cell density
VHH	single-domain antibody
VNT	virus neutralization test
VSV	vesicular stomatitis virus
ZAPI	Zoonoses Anticipation and Preparedness Initiative

## Acknowledgments

The authors would like to thank Dr. Michèle Bouloy (Institut Pasteur, France) who kindly provided the RVFV Clone 13. We also would like to thank all partners, scientists, post-docs, and graduate students involved in the ZAPI Project for their work and contributions, in particular: Paul Varley, Dorota Kozub, Gary Pettman, Maiken Kristiansen, Aled Charles, Kieran Mistry, Ainul Zulkepli, Stephanie Davies, Katie Day, Sofia Ekizoglou, Peng Ke, Bradley Rawlins, Evangelia Ttofí, Tom Witkos, Chloe Parry (AstraZeneca), Sandra van de Water (Wageningen Bioveterinary Research, the Netherlands) and Jean-Christophe

## Disclosure statement

B.J.B. is an inventor on a patent application on monoclonal antibodies targeting MERS-CoV including the antibodies MERS-7.7G6 and MERS-1.6C7 (patent publication no.: WO/2020/169755). S.R.C., S.I., V.L., L.A., A.T., U.O., L.K., K.M., M.H., O.D work for AstraZeneca and may own AstraZeneca stocks. No other potential conflict of interest was reported by the authors.

## Funding

This study was financed by a grant from the Zoonotic Anticipation and Preparedness Initiative (ZAPI) project; which was funded by the Innovative Medicines Initiative (IMI, grant agreement no. 115760), the European Commission, and in-kind contributions from European Federation of Pharmaceutical Industries and Associations (EFPIA) partners.

## ORCID

Berend-Jan Bosch  <http://orcid.org/0000-0002-3864-232X>

## References

- Rajendra Y, Hougland MD, Alam R, Morehead TA, Barnard GC. A high cell density transient transfection system for therapeutic protein expression based on a CHO GS-knockout cell line: process development and product quality assessment. *Biotechnol Bioeng.* 2015;112:977–86. doi:10.1002/bit.25514.
- Steger K, Brady J, Wang W, Duskin M, Donato K, Peshwa M. CHO-S antibody titers >1 gram/liter using flow electroporation-mediated transient gene expression followed by rapid migration to high-yield stable cell lines. *J Biomol Screen.* 2015;20:545–51. doi:10.1177/1087057114563494.
- Dumont J, Euwart D, Mei B, Estes S, Kshirsagar R. Human cell lines for biopharmaceutical manufacturing: history, status, and future perspectives. *Crit Rev Biotechnol.* 2016;36:1110–22. doi:10.3109/07388551.2015.1084266.
- Ye J, Kober V, Tellers M, Naji Z, Salmon P, Markusen JF. High-level protein expression in scalable CHO transient transfection. *Biotechnol Bioeng.* 2009;103:542–51. doi:10.1002/bit.22265.
- Kim JY, Kim YG, Lee GM. CHO cells in biotechnology for production of recombinant proteins: current state and further potential. *Appl Microbiol Biotechnol.* 2012;93:917–30. doi:10.1007/s00253-011-3758-5.
- Gutierrez-Granados S, Cervera L, Kamen AA, Godia F. Advancements in mammalian cell transient gene expression (TGE) technology for accelerated production of biologics. *Crit Rev Biotechnol.* 2018;38:918–40. doi:10.1080/07388551.2017.1419459.
- Daramola O, Stevenson J, Dean G, Hatton D, Pettman G, Holmes W, Field R. A high-yielding CHO transient system: co-expression of genes encoding EBNA-1 and GS enhances transient protein expression. *Biotechnol Prog.* 2014;30:132–41. doi:10.1002/btpr.1809.
- Schmitt MG, White RN, Barnard GC. Development of a high cell density transient CHO platform yielding mAb titers greater than 2 g/L in only 7 days. *Biotechnol Prog.* 2020;36:e3047. doi:10.1002/btpr.3047.
- Stuible M, Burlacu A, Perret S, Brochu D, Paul-Roc B, Baardsnes J, Loignon M, Grazzini E, Durocher Y. Optimization of a high-cell-density polyethylenimine

- transfection method for rapid protein production in CHO-EBNA1 cells. *J Biotechnol.* 2018;281:39–47. doi:10.1016/j.jbiotec.2018.06.307.
10. Lee JH, Hansen HG, Park SH, Park JH, Kim YG. Transient gene expression-based protein production in recombinant mammalian cells. In Lee GM, Fastrup H, Yup KS, Nielsen LJ, Stephanopoulos G, editors. *Cell culture engineering: recombinant protein production*. KGaA, Boschstr. (Weinheim, Germany): Wiley-VCH Verlag GmbH & Co; 2019. p. 49–72. doi:10.1002/9783527811410.
  11. Pham PL, Perret S, Doan HC, Cass B, St-Laurent G, Kamen A, Durocher Y. Large-scale transient transfection of serum-free suspension-growing HEK293 EBNA1 cells: peptone additives improve cell growth and transfection efficiency. *Biotechnol Bioeng.* 2003;84:332–42. doi:10.1002/bit.10774.
  12. Durocher Y, Perret S, Kamen A. High-level and high-throughput recombinant protein production by transient transfection of suspension-growing human 293-EBNA1 cells. *Nucleic Acids Res.* 2002;30:e9. doi:10.1093/nar/30.2.e9.
  13. Geisse S, Henke M. Large-scale transient transfection of mammalian cells: a newly emerging attractive option for recombinant protein production. *J Struct Funct Genomics.* 2005;6:165–70. doi:10.1007/s10969-005-2826-4.
  14. Raymond C, Tom R, Perret S, Moussouami P, L'Abbe D, St-Laurent G, Durocher Y. A simplified polyethylenimine-mediated transfection process for large-scale and high-throughput applications. *Methods.* 2011;55:44–51. doi:10.1016/j.ymeth.2011.04.002.
  15. Tuveesson O, Uhe C, Rozkov A, Lullau E. Development of a generic transient transfection process at 100 L scale. *Cytotechnology.* 2008;56:123–36. doi:10.1007/s10616-008-9135-2.
  16. Tyzack E, Pettman G, Daramola L. Abstracts from the 25th European society for animal cell technology meeting: cell technologies for innovative therapies. *BMC Proc.* 2018;12:061. doi:10.1186/s12919-018-0097-x.
  17. Stuible M, van Lier F, Croughan MS, Durocher Y. Beyond pre-clinical research: production of CHO-derived biotherapeutics for toxicology and early-phase trials by transient gene expression or stable pools. *Curr Opin Chem Eng.* 2018;22:145–51. doi:10.1016/j.coche.2018.09.010.
  18. Kelley B. Developing therapeutic monoclonal antibodies at pandemic pace. *Nat Biotechnol.* 2020;38:540–45. doi:10.1038/s41587-020-0512-5.
  19. Schellekens H, Aldosari M, Talsma H, Mastrobattista E. Making individualized drugs a reality. *Nat Biotechnol.* 2017. doi:10.1038/nbt.3888.
  20. Widjaja I, Wang C, van Haperen R, Gutiérrez-Álvarez J, van Dieren B, Okba NMA, Raj VS, Li W, Fernandez-Delgado R, Grosveld F, et al. Towards a solution to MERS: protective human monoclonal antibodies targeting different domains and functions of the MERS-coronavirus spike glycoprotein. *Emerg Microbes Infect.* 2019;8:516–30. doi:10.1080/22221751.2019.1597644.
  21. Wichgers Schreur PJ, van de Water S, Harmsen M, Bermudez-Mendez E, Drabek D, Grosveld F, Wernike K, Beer M, Aebischer A, Daramola O, et al. Multimeric single-domain antibody complexes protect against bunyavirus infections. *Elife.* 2020;9. doi:10.7554/eLife.52716.
  22. Wang C, van Haperen R, Gutierrez-Alvarez J, Li W, Okba NMA, Albulescu I, Widjaja I, van Dieren B, Fernandez-Delgado R, Sola I, et al. A conserved immunogenic and vulnerable site on the coronavirus spike protein delineated by cross-reactive monoclonal antibodies. *Nat Commun.* 2021;12:1715. doi:10.1038/s41467-021-21968-w.
  23. Jain NK, Barkowski-Clark S, Altman R, Johnson K, Sun F, Zmuda J, Liu CY, Kita A, Schulz R, Neill A, et al. A high density CHO-S transient transfection system: comparison of ExpiCHO and Expi293. *Protein Expr Purif.* 2017;134:38–46. doi:10.1016/j.pep.2017.03.018.
  24. Sousa F, Prazeres DM, Queiroz JA. Improvement of transfection efficiency by using supercoiled plasmid DNA purified with arginine affinity chromatography. *J Gene Med.* 2009;11:79–88. doi:10.1002/jgm.1272.
  25. USA, FDA. Guidance for Industry: considerations for plasmid DNA vaccines for infectious disease indications. *Biotechnol Law Rep.* 2007;26:641–48. doi:10.1089/blr.2007.9905.
  26. Brunner M, Fricke J, Kroll P, Herwig C. Investigation of the interactions of critical scale-up parameters (pH, pO<sub>2</sub> and pCO<sub>2</sub>) on CHO batch performance and critical quality attributes. *Bioprocess Biosyst Eng.* 2017;40:251–63. doi:10.1007/s00449-016-1693-7.
  27. Chi B, Veyssier C, Kasali T, Uddin F, Sellick CA. At-line high throughput site-specific glycan profiling using targeted mass spectrometry. *Biotechnol Rep (Amst).* 2020;25:e00424. doi:10.1016/j.btre.2020.e00424.
  28. Kim J, Albarghouthi M. Rapid monitoring of high-mannose glycans during cell culture process of therapeutic monoclonal antibodies using lectin affinity chromatography. *J Sep Sci.* 2022. doi:10.1002/jssc.202100903.
  29. Robinson DK, Chan CP, Yulp C, Tsai PK, Tung J, Seamans TC, Lenny AB, Lee DK, Irwin J, Silberklang M. Characterization of a recombinant antibody produced in the course of a high yield fed-batch process. *Biotechnol Bioeng.* 1994;44:727–35. doi:10.1002/bit.260440609.
  30. Pacis E, Yu M, Autsen J, Bayer R, Li F. Effects of cell culture conditions on antibody N-linked glycosylation—what affects high mannose 5 glycoform. *Biotechnol Bioeng.* 2011;108:2348–58. doi:10.1002/bit.23200.
  31. Bolisetty P, Tremml G, Xu S, Khetan A. Enabling speed to clinic for monoclonal antibody programs using a pool of clones for IND-enabling toxicity studies. *MAbs.* 2020;12:1763727. doi:10.1080/19420862.2020.1763727.
  32. Gahn TA, Sugden B. An EBNA-1-dependent enhancer acts from a distance of 10 kilobase pairs to increase expression of the Epstein-Barr virus LMP gene. *J Virol.* 1995;69:2633–36. doi:10.1128/JVI.69.4.2633-2636.1995.
  33. Muller R, Saluzzo JF, Lopez N, Dreier T, Turell M, Smith J, Bouloy M. Characterization of clone 13, a naturally attenuated avirulent isolate of Rift Valley fever virus, which is altered in the small segment. *Am J Trop Med Hyg.* 1995;53:405–11. doi:10.4269/ajtmh.1995.53.405.
  34. Wichgers Schreur PJ, Paweska JT, Kant J, Kortekaas J. A novel highly sensitive, rapid and safe Rift Valley fever virus neutralization test. *J Virol Methods.* 2017;248:26–30. doi:10.1016/j.jviromet.2017.06.001.